Controlled selectivity through reversible inhibition of the catalyst: Stereodivergent semihydrogenation of alkynes

Jie Luo,[1,3] Yaoyu Liang,[1,3] Michael Montag,[1] Yael Diskin-Posner,[2] Liat Avram,[2] David Milstein[1,*]

[1]Department of Molecular Chemistry and Materials Science and [2]Department of Chemical Research Support, Weizmann Institute of Science, Rehovot, 76100, Israel. [3]These authors contributed equally to this work.
*E-mail: david.milstein@weizmann.ac.il

SUMMARY

Catalytic semihydrogenation of internal alkynes using H_2 is an attractive atom-economical route to various alkenes, and its stereocontrol has received widespread attention, both in homogeneous and heterogeneous catalysis. Herein, a novel strategy is introduced, whereby a poisoning catalytic thiol is employed as a reversible inhibitor of a ruthenium catalyst, resulting in the first controllable H_2-based semihydrogenation of internal alkynes. Both (E)- and (Z)-alkenes were obtained efficiently and highly-selectively, under very mild conditions, using a single homogenous acridine-based ruthenium catalyst. Mechanistic studies indicate that the (Z)-alkene is the reaction intermediate leading to the (E)-alkene, and that addition of a catalytic amount of bidentate thiol impedes the Z-E isomerization step by forming stable ruthenium thiol(ate) complexes, while still allowing the main hydrogenation reaction to proceed. Thus, the absence or presence of catalytic thiol controls the stereoselectivity of this alkyne semihydrogenation, affording either the (E)-isomer as the final product, or halting the reaction at the (Z)-intermediate. The developed system, which is also applied to the controllable isomerization of a terminal alkene, demonstrates how selective metal catalysis can be achieved by reversible inhibition of the catalyst with a simple auxiliary additive.

INTRODUCTION

Most catalytic reactions involve *in-situ* generated intermediates, which are usually quite reactive under the reaction conditions and are thus seldom isolated as products (Figure 1a).[1-2] For example, the *trans*-selective catalytic semihydrogenation of alkynes typically begins with *cis*-hydrogenation, but the generated (Z)-alkene is only a kinetic intermediate, which is then rapidly isomerized into the thermodynamically more stable (E)-alkene product (Figure 1b).[3-9] If a strategy can be devised to slow down a specific reaction step, such as the Z-to-E isomerization in the *trans*-semihydrogenation of alkynes, the reactive intermediates can be stabilized, and may even be isolable as end-products from the same system, which would be of great interest and is highly-advantageous. Nevertheless, the state-of-the-art methodologies to selectively access both (E)- and (Z)-alkenes rely on the transfer-semihydrogenation of alkynes using different catalysts.[10-16] Some strategies involve the use of additives in order to switch the stereoselectivities of these transformations,[17-20] but their mechanisms are unclear and they are still limited to transfer-semihydrogenation with H_2 surrogates, and also usually require stoichiometric amounts of additives, which inevitably generates waste and is neither atom-economical nor sustainable.

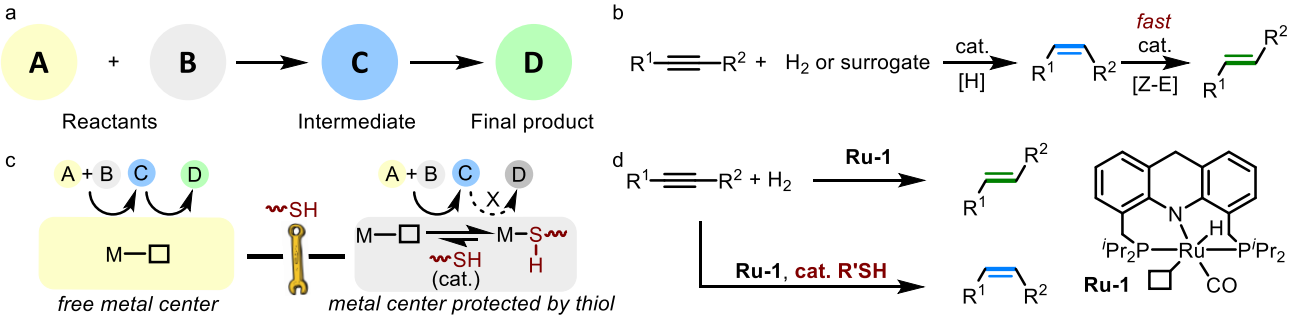

Figure 1. Controllable E/Z semihydrogenation of alkynes enabled by the poisoning effect of thiol. (a) Stepwise reactions involving the generation of intermediates. (b) Typical *trans*-selective semihydrogenation of alkynes to access E-alkenes. (c) Controlled selectivity through reversible inhibition of the catalyst by thiol. (d) This work.

Thiol(ate)s are known to have very strong intrinsic affinity to transition metals, and are therefore widely used as ligands,[21-24] biological inhibitors,[25-26] metal ion probes[27-29] and the end groups of self-assembled monolayers.[30-31] However, in transition metal catalysis, this strong affinity of thiol(ate)s is usually problematic, since it can easily poison the catalysts by blocking their metal centers.[32-38] For example, this poisoning effect of thiols could quench the active Au sites dispersion in supported Au nanoparticles used for benzyl alcohol oxidation.[38] Nevertheless, coordinated thiols can dissociate from metal centers and be displaced by other ligands.[39] Thus, we wondered whether adding a catalytic amount of thiol to a reaction mixture containing a given transition-metal-based catalyst could afford a protected form of this catalyst *in situ*, with the thiol acting as a reversible inhibitor of the catalyst. Ideally, this thiol protecting group would selectively open the coordination site only for targeted molecules, such as alkynes, and thus efficiently impede other unwanted reactions.[40-46] In this manner, the simple addition of thiol could serve as a switch to control the selectivity of reactions by reversibly protecting the metal center (Figure 1c).

Herein, we demonstrate the use of thiol poisoning as an effective means of achieving controllable semihydrogenation of alkynes with H_2, in a process that is homogeneously catalyzed by an acridine-based PNP-type ruthenium complex under very mild conditions (Figure 1d). In the absence of thiol, this system enables the highly efficient *trans*-selective semihydrogenation of internal alkenes into E-alkenes, while in the presence of a catalytic amount of thiol it selectively affords Z-alkenes.

RESULTS AND DISCUSSION

Establishment and optimization of the catalytic reaction conditions. Catalytic semihydrogenation of internal alkynes is an attractive route to access different alkenes for small-scale laboratory synthesis as well as large-scale industrial processes.[46-61] Controlling the stereoselectivity and avoiding the formation of over-reduced alkane products are two major challenges facing the development of such reactions. The acridine-based PNP-type ruthenium pincer complex **Ru-1** was found to be a highly active catalyst for the *trans*-semihydrogenation of alkynes. For example, in the presence of 0.4 mol% **Ru-1**, 0.25 mmol of diphenylacetylene (**1a**) in 0.5 mL of toluene-d_8 was fully hydrogenated into (E)-stilbene within only 15 min at room temperature, inside a 3 mL J. Young NMR tube pressurized with 5 bar of hydrogen gas (2 equiv; Figure 2a). This translates into a TOF of more than 1000 h^{-1}, which, to the best of our knowledge, represents the most efficient *trans*-semihydrogenation of any alkyne reported to date.[3-20, 46-61] As the reaction progressed, a clear color change from brown-red to yellow was observed, with the latter being that of **Ru-1**, and this visible change could be used as a reaction indicator.[7] Notably, only negligible over-reduction into alkane **3a** was observed (<1 %), possibly due to the very mild conditions employed.

The progress of the semihydrogenation reaction was monitored by NMR spectroscopy in order to extract the kinetic profiles of the various reaction components (Figure 2b, see SI for procedures). Based on the measured data, **1a** was found to be consumed immediately upon introduction of H_2, with no significant induction period, indicating the facile generation of the catalytically active species in this system. Moreover, (Z)-**2a** was observed to accumulate as the kinetic product, and then be consumed as the NMR signals of its stereoisomer (E)-**2a** began to appear, suggesting that (E)-**2a** was being generated from (Z)-**2a** by Z-E isomerization. It should be noted that the rate in which (E)-**2a** was generated increased as the reaction progressed, with most of (Z)-**2a** being converted into (E)-**2a** within a very short interval near the end of the reaction. This presumably occurs after full conversion of the alkyne, thus indicating that the presence of alkyne impedes the isomerization step. These results also imply that in the absence of alkyne, **Ru-1** is a highly efficient catalyst for Z-E isomerization.

Given the above observations, it is likely that (Z)-alkene isomerization occurs at the vacant site of **Ru-1**, and molecules with higher affinity to the metal center, such as alkynes, are able to block this coordination site and thereby impede the isomerization process.[20] However, the selectivity of the reaction toward (Z)-**2a** quickly dropped once alkyne conversion reached 50% (see the Z/E curve in Figure 2b), and completely inverted at the end of the reaction. This prompted us to search for an auxiliary additive, which could coordinate to the metal center in a way that would allow the main reaction to take place while impeding the isomerization step, and thereby effectively halting the reaction at intermediate (Z)-**2a**.

To pursue this idea, we first examined the effect of oxygen-containing additives, such as methanol and benzoic acid (Figure 2c). Employing methanol as either an additive (0.5 mol%) or solvent resulted in full conversion of **1a** into (E)-**2a**, whereas 1.25 equiv of benzoic acid (per catalyst) strongly inhibited the reaction, leading to less than 5% hydrogenation products after 10 h. In the latter case, it was found that a ruthenium-carboxylate complex[62-63] was easily generated in the reaction mixture, but this species could not effectively activate H_2 gas to regenerate the ruthenium hydride species (see Figure S24), which may account for the sluggish nature of the catalytic reaction in the presence of benzoic acid. Amines were also examined, since they are expected to bind more tightly to the ruthenium center than oxygen-based additives. Interestingly, when 0.5 mol% hexylamine ($HexNH_2$) was added along with the catalyst, 4% of (Z)-**2a** was observed by the end of the reaction, after full conversion of **1a** had been reached. This result supported our assumption that additives with higher metal affinity would improve the yield of the (Z)-**2a** intermediate obtained after completion of the reaction.

However, a further screening of different amine additives failed to improve the yield of (Z)-**2a** under similar reaction conditions (see Figure S32 for the screened amines).

Based on these preliminary results, it was decided to explore thiol additives, since they are known to strongly coordinate to Ru(II) centers. Nevertheless, ruthenium thiolate complexes that may be generated during the reaction are expected to readily activate H_2, thereby regenerating the catalytically-active ruthenium hydride species, as we have recently observed.[64] Initially, 0.5 mol% of 1-hexanethiol (HexSH) was added to the reaction mixture under catalytic conditions similar to the previous experiments, but (E)-**2a** still formed as the only product. This indicated that HexSH is compatible with the hydrogenation reaction, but is not effective enough as a catalyst inhibitor to impede the alkene isomerization process. Thus, various other thiols were screened, showing significant variations in the results. For example, when *N*-decyl 2-mercaptoacetamide (2-MAA) or ethanedithiol (EDT) were used as additives, no alkyne conversion was observed, but when butyl 3-mercaptopropionate (3-MPA) was employed, (Z)-**2a** was obtained in 49% yield, with a Z/E selectivity of 1:1. The different behavior of these thiols may be due to their tethered functional groups, which was not observed in the amine additives with similar structures (See Figure S32). Significantly, the best result was obtained when a cysteine derivative, *N*-acetylcysteine ethyl ester (NACET), was used, allowing us to improve the Z/E selectivity to 9:1, and achieve a yield of 87% for (Z)-**2a**, with 96% alkyne conversion.

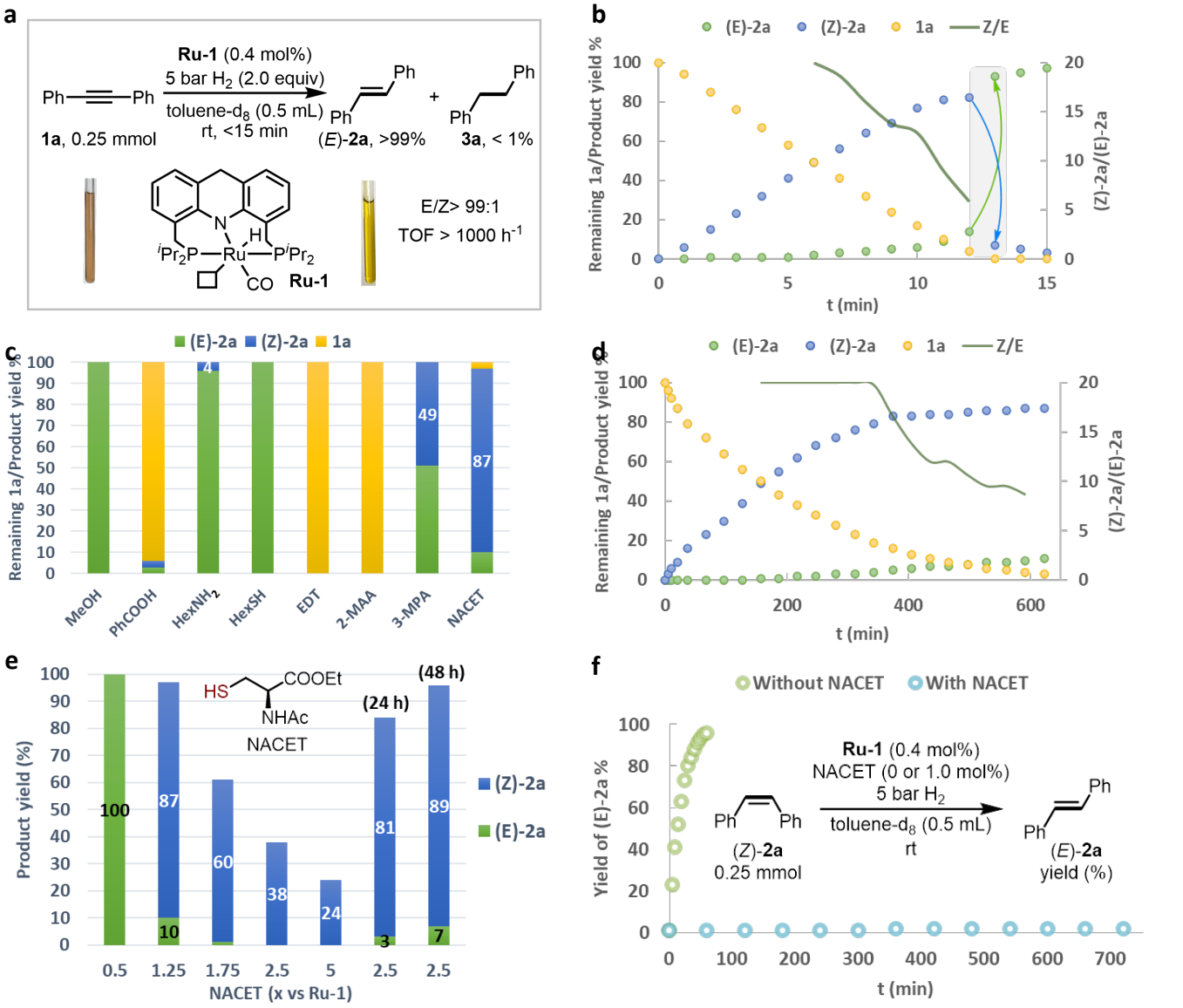

Figure 2. Aspects of controllable E/Z semihydrogenation of alkynes catalyzed by Ru-1. (a) *Trans*-semihydrogenation of **1a** catalyzed by **Ru-1**. (b) Kinetic profile of the *trans*-semihydrogenation of **1a**. (c) Additive screening under conditions similar to Figure 2a, with 0.5 mol% additive, 10 h. (d) Kinetic profile of the *cis*-semihydrogenation of **1a** in the presence of NACET. (e) Effect of the amount of added NACET on the selectivity of the semihydrogenation reaction, after 10 h of reaction time unless noted otherwise. (f) Control experiments for the Z-E isomerization process.

To gain further insights into the effect of NACET, we monitored the progress of the catalytic process in the presence of this additive by NMR spectroscopy, and constructed the corresponding kinetic profiles (Figure 2d). As indicated by the kinetic curves, despite the presence of thiol in the catalytic mixture, the reaction proceeded smoothly, exhibiting no induction period and reaching high conversion, with 87% of (Z)-**2a** being generated within 10 h. Prolonging the reaction time to 20 h had no significant deleterious effect on the yield of (Z)-**2a**, with 82% being detected in solution, alongside full conversion of **1a**. It should be noted that alkene isomerization does occur in the presence of thiol, but it is efficiently slowed down during the whole process (see the Z/E curve in Figure 2d). These results prompted us to investigate another important aspect of the NACET additive, namely, the influence of its amount relative to the catalyst **Ru-1** (Figure 2e). As expected, 0.5 equiv of NACET did not prevent the isomerization of (Z)-**2a**, resulting in full conversion of **1a** into (E)-**2a**. Increasing the relative amount of thiol decreased the hydrogenation rate, as is evident from the significant drop in product yield, and this largely rules out an outer-sphere hydrogenation mechanism, which does not involve alkyne coordination to the metal center (also see Figure S28). At the same time, the selectivity of the reaction greatly benefits from increasing the amount of thiol. Thus, the catalytic reaction employing 2.5 equiv of NACET relative to **Ru-1** gave 84% of **2a** after 24 h, with an excellent Z/E selectivity of 27:1. Prolonging the reaction time to 48 h improved the yield of **2a**, but reduced the selectivity (96%, Z/E = 13:1).

The effect of NACET on the rate of Z-E isomerization catalyzed by **Ru-1** was assessed by using (Z)-**2a** as the substrate, and monitoring its conversion into the E isomer in toluene-d_8 under 5 bar of H_2, in the absence and presence of the thiol, using *in situ* NMR spectroscopy (Figure 2f). The isomerization rates in these control experiments were slower than in the actual catalytic runs, possibly because of the easier access of the catalytically active species in the presence of alkyne substrate (see Note S1 for details). Nevertheless, the remarkable effect of thiol-induced inhibition on the isomerization process is clearly apparent. Thus, in the absence of thiol, 96% of (Z)-**2a** were converted into (E)-**2a** within 1 h, whereas in the presence of 1 mol% NACET, the isomerization rate dropped by a factor of >500, resulting in less than 2% conversion after 12 h. Therefore, this thiol can serve as a highly-reliable catalytic inhibitor, which prevents interactions between alkenes and the metal center in this catalytic system.

Mechanistic investigations. The catalytic species involved in the controllable E/Z semihydrogenation described above were investigated in detail, in order to better understand the reaction mechanism. When **Ru-1** was mixed with 1 equiv of alkyne **1a** in benzene or toluene, a new species appeared in the $^{31}P\{^1H\}$ NMR spectrum upon standing at room temperature, as the signal belonging to **Ru-1** diminished. This species exhibited a very broad NMR signal, ranging from 79 to 105 ppm, which indicates fluxional behavior. Interestingly, when the temperature of the toluene solution was lowered to -40 °C, the broad peak split into two distinct resonances at 76.3 and 95.6 ppm (Figure S10), indicating loss of molecular symmetry. Moreover, no hydride peak was observed for the new species in the ^1H NMR spectrum, but a triplet at 5.2 ppm was detected, attributable to a vinylic hydrogen atom. These observations are consistent with the structure of the ruthenium alkenyl complex **Ru-2**, featuring a facially-coordinated pincer ligand (Figure 3a). It should be noted that generation of this alkenyl species in solution was accompanied by a color change to red-brown, as is also observed during the initial stages of the catalytic reaction (Figure 2a). **Ru-2** was found to be unstable at room temperature in solution, gradually decomposing into a mixture of unidentified species, but in the presence of 5 bar H_2, this complex quickly converted back into **Ru-1** at room temperature, with concomitant generation of (E)-**2a**. These results clearly indicate that the alkenyl species **Ru-2** is a reaction intermediate in the semihydrogenation of alkynes. In an attempt to also investigate the reactivity of **Ru-1** toward alkenes, we mixed this complex with either (Z)- or (E)-**2a**, but no new species were observed in solution. Instead, the $^{31}P\{^1H\}$ NMR spectra of these reaction mixtures only exhibited line broadening of the **Ru-1** peak, and this likely indicates a weak π-interaction between the alkenes and Ru center.

In contrast to **Ru-1**, the aromatized complex **Ru-3** does not react with alkyne **1a** at room temperature, and shows no catalytic activity vis-à-vis alkyne hydrogenation. Thus, when the semihydrogenation of alkyne **1a** was attempted with **Ru-3** under the same conditions used for **Ru-1**, no reaction was observed. **Ru-3** was also found to be unable to catalyze the Z-E isomerization of (Z)-**2a** (Figure 3b). Furthermore, using other ruthenium catalysts developed by our group for the hydrogenation of polar carbonyl groups, either very poor reactivity or selectivity was observed under the typical alkyne hydrogenation conditions (See Figure S31). These results highlight the unique reactivity of **Ru-1**, which may be ascribed to its readily available vacant site, as well as increased reactivity of its hydride toward alkynes, compared to other catalysts.

The catalytic species generated during alkene semihydrogenation in the presence of NACET were also monitored by NMR spectroscopy in toluene. No detectable amounts of **Ru-1** or **Ru-2** were found in solution, but a new ruthenium complex was observed as the predominant species. This complex could be obtained independently by mixing **Ru-1** with NACET,[36, 64-66] and was characterized by NMR spectroscopy as the ruthenium-hydrido-thiol complex **Ru-4** (Figure 3c). When the solution containing this complex was heated at 100 °C for 10 min, a Ru-thiolate complex formed, accompanied by the release of H_2 gas. However, in contrast to complex **Ru-5**, which contains a monodentate thiolate ligand and was previously reported as the reaction product of **Ru-1** and hexanethiol,[64] the new thiolate complex, obtained with NACET, was identified as **Ru-6**, in which the thiolate ligand is coordinated in a bidentate mode. Importantly, **Ru-6** was also observed in the actual catalytic runs, albeit in small amounts, implying that it is a reaction intermediate (See Figure S26). The exact structure of **Ru-6** was confirmed by an X-ray analysis of its analog **Ru-6'**, which was prepared from **Ru-1** and butyl 3-mercaptopropionate using

the same procedure (Figure 3d). Interestingly, the coordinatively saturated **Ru-6** was shown to activate H_2 at room temperature to regenerate the ruthenium hydride species **Ru-4**, and this reaction may be essential for ensuring catalytic turnover in our system (Figure S27).

The bidentate coordination of the thiolate ligand in **Ru-6** is expected to stabilize this intermediate. The transformation of **Ru-1** to **Ru-6** was computationally studied by density functional theory (DFT) calculations using toluene as the model solvent, demonstrating that the generation of **Ru-6** is indeed the overall thermodynamically favorable outcome, to the extent of 7.1 kcal/mol (Figure 3e).[66] It should also be noted that in a nonpolar solvent such as toluene, **Ru-6** (as well as **Ru-4**) can be further stabilized by hydrogen bonding between the amide groups of the coordinated and free NACET units, as computationally modeled in the gas phase (Figure S86). In the actual catalysis, the stabilizing effects of NACET can drive the reaction forward to generate **Ru-6**, and may account for the enhanced selectivity observed with NACET as additive, compared to the other examined thiols (Figure 3e). Moreover, **Ru-6** may also be generated during the catalytic reaction by direct protonation of the alkenyl species **Ru-2** by an incoming thiol, as shown by a control experiment (Figure 3f). This also implies that the acidity of the thiol[67-68] is essential for quenching **Ru-2** to avoid its hydrogenolysis back to **Ru-1**, which is responsible for the Z-E isomerization of alkenes (also see Note S2).

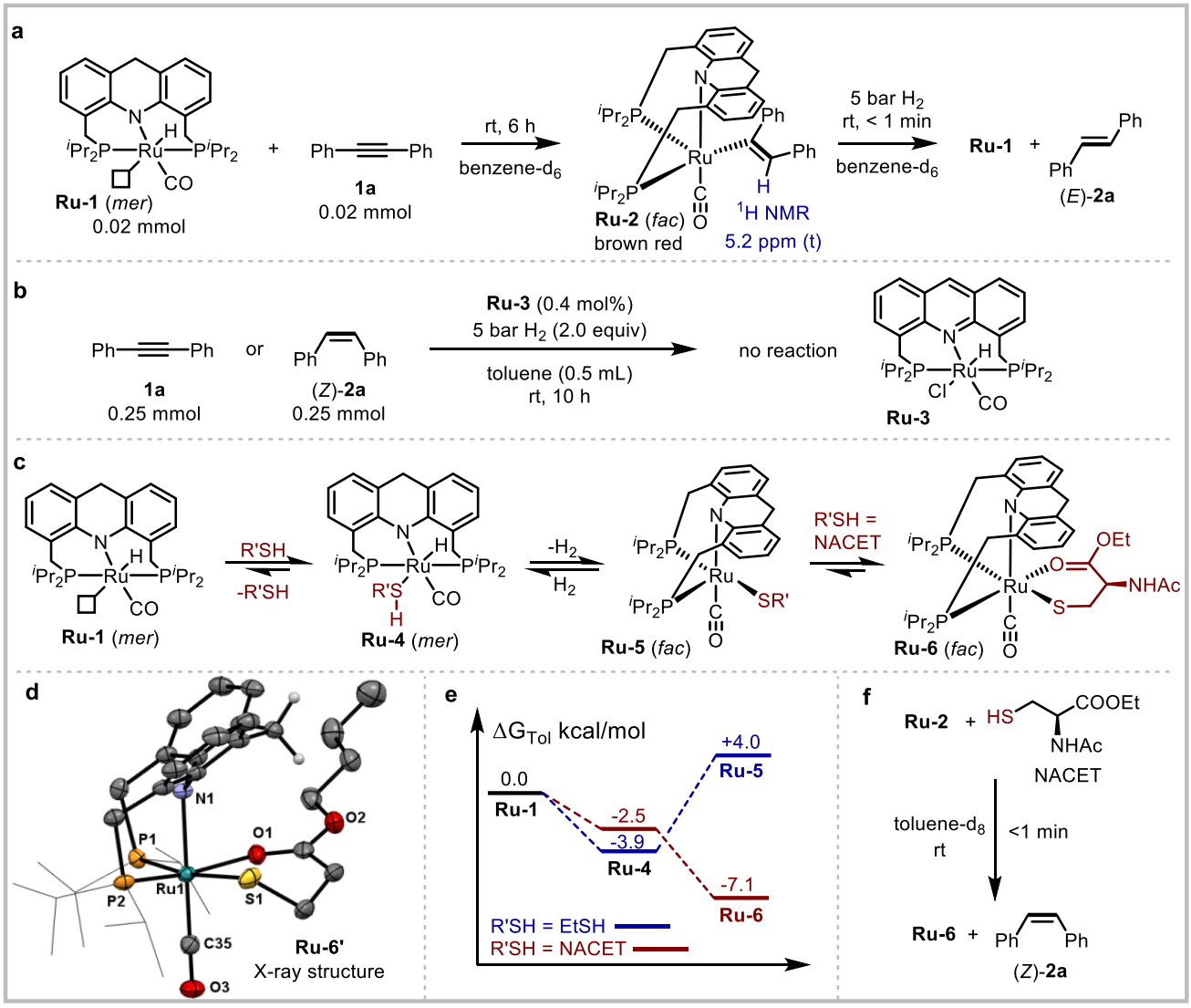

Figure 3. Mechanistic studies involving different steps of the reaction. (a) Generation of a ruthenium alkenyl species. (b) Control experiments using **Ru-3** as the catalyst. (c) Reactions between **Ru-1** and NACET. (d) X-ray crystal structure of **Ru-6'**, with isopropyl groups presented in wireframe style and most hydrogen atoms omitted for clarity. (e) Calculated potential energy surface of different catalytically-relevant ruthenium species. (f) Transformation of **Ru-2** to **Ru-6** with NACET.

Proposed mechanism. Based on the above results, a mechanism is proposed for the controllable semihydrogenation of alkynes in the current catalytic system. According to our previous studies, as well as the current results (see Notes S1 and S2), *fac*-**Ru-1** is probably the actual catalytically-active species (step i), which is generated from **Ru-1** through a ring flip, and exhibits a vacant coordination site *cis* to the hydride ligand.[69-70] Initially, the alkyne inserts into the Ru-H bond to generate

the alkenyl species **Ru-2** (steps ii and iii), which was fully characterized by NMR spectroscopy as part of the control experiments. Subsequently, this species can heterolytically split H_2 to regenerate the ruthenium hydride species *fac*-**Ru-1** and release the (Z)-alkene product (kinetic intermediate, step iv). The latter can then further interact with the ruthenium center to undergo Z-E isomerization, thereby affording the final (E)-alkene product (thermodynamic product, step v). In the presence of thiol, the ruthenium species are poisoned through formation of stable ruthenium thiol(ate) complexes (**Ru-4** and **Ru-6**, step vi to ix). In this manner, the thiol serves as a reversible inhibitor protecting the vacant site on the metal center. The affinity of the alkyne is high enough so that it is able to exchange with the thiol and insert into the Ru-H bond (step vii, ii and iii), thereby generating the ruthenium alkenyl species **Ru-2**, which can then be protonated by the thiol to form **Ru-6** along with the release of the (Z)-alkene (step ix). By contrast, the generated alkenes, which have much lower affinities to the metal center than the alkyne or thiol, do not interact further with the ruthenium center, as verified by the control experiments that directly investigated Z-E isomerization (Figure 2f). Notably, in the actual catalytic runs, the thiol not only impeded Z-E isomerization, but also slowed down the reaction after significant alkyne conversion had been reached, thus pausing the reaction at the (Z)-intermediate stage and leading to excellent selectivity. While the added thiol is responsible for the selectivity of the reaction, its role in promoting H_2 activation by the ruthenium thiolate complex to regenerate the Ru-H intermediate is also essential to ensure further turnover of the entire catalytic cycle.

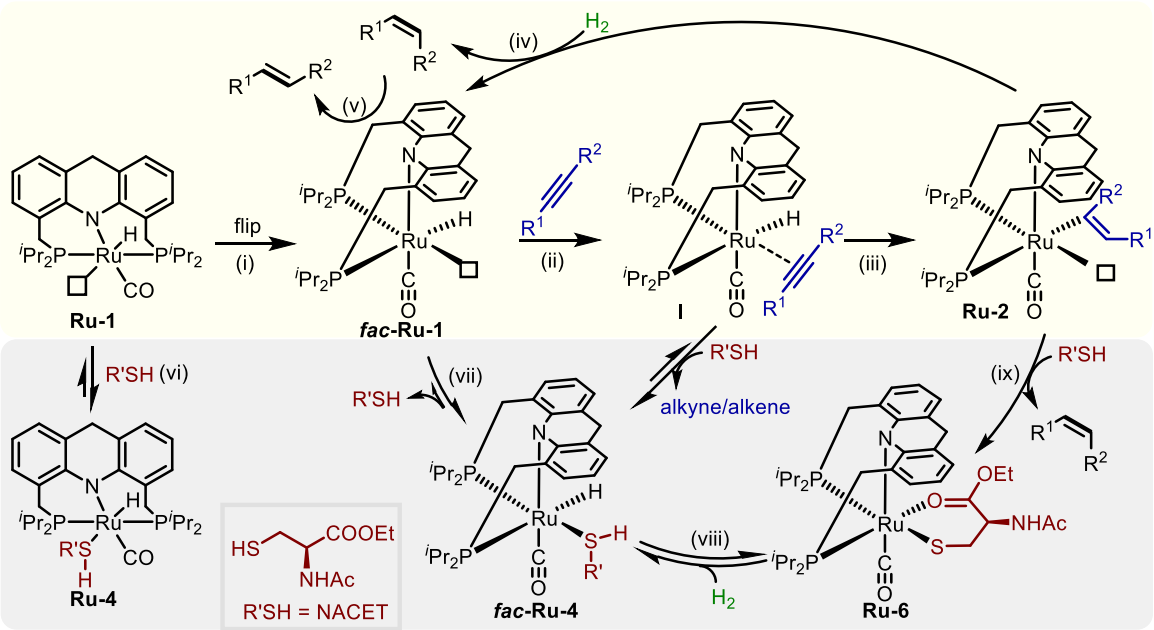

Figure 4. Proposed catalytic cycle for the semihydrogenation of alkynes in the absence and presence of thiol.

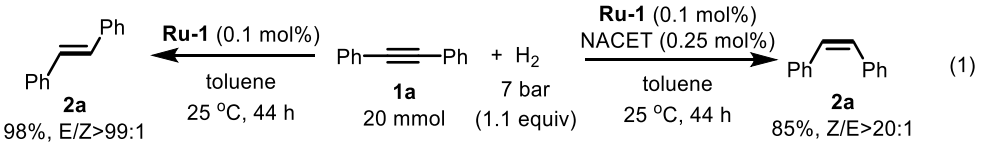

Substrate scope. The practicality of our catalytic system was also examined. Firstly, the procedure was scaled up to involve 20 mmol of alkyne in a 90 mL Fischer-Porter tube, resulting in the efficient formation of both (E)- and (Z)-**2a** using only 0.1 mol% of **Ru-1** in the absence or presence of a catalytic amount of the NACET additive (eq. 1). Notably, no significant amounts of **3a** were observed in either case, demonstrating that this system efficiently suppresses the unwanted over-reduction reaction. Subsequently, the substrate scope of this catalytic reaction was explored, generally using 0.5 mmol of substrate under 1 bar of H_2 at room temperature, and employing 0.2 mol% **Ru-1** (Figure 5, see Table S1 for detailed conditions). It was found that substituents at different positions around the phenyl rings of diphenylacetylene did not affect the results, and the effect of thiol on these stereodivergent semihydrogenations was preserved, thereby allowing excellent selectivities to be achieved (**2b**-**2d**). The developed system was also found to be compatible with a wide range of functional groups. Thus, substituents like halogen atoms, bulky ^{t}Bu group, electron-donating OMe group, electron-withdrawing CF_3 group, and even ester, secondary amide, and tertiary amine groups, were all well tolerated (**2e**-**2m**). Alkynes bearing other aryl moieties, such as naphthalene and thiophene, were also suitable substrates (**2n**, **2o**). In addition to these diaryl internal alkynes, triple C≡C bonds with aliphatic substituents were also explored (**1p**-**1r**). These substrates usually exhibit higher reactivities, possibly due to decreased steric hindrance. Our controllable

semihydrogenation methodology was also applied to phenyl acetylene **1s** under similar reaction conditions, resulting in a chemoselective hydrogenation. Interestingly, direct hydrogenation to alkane **3s** was observed in the absence of thiol, whereas addition of a catalytic amount of NACET allowed us to obtain styrene **2s** in >20:1 chemoselectivity.

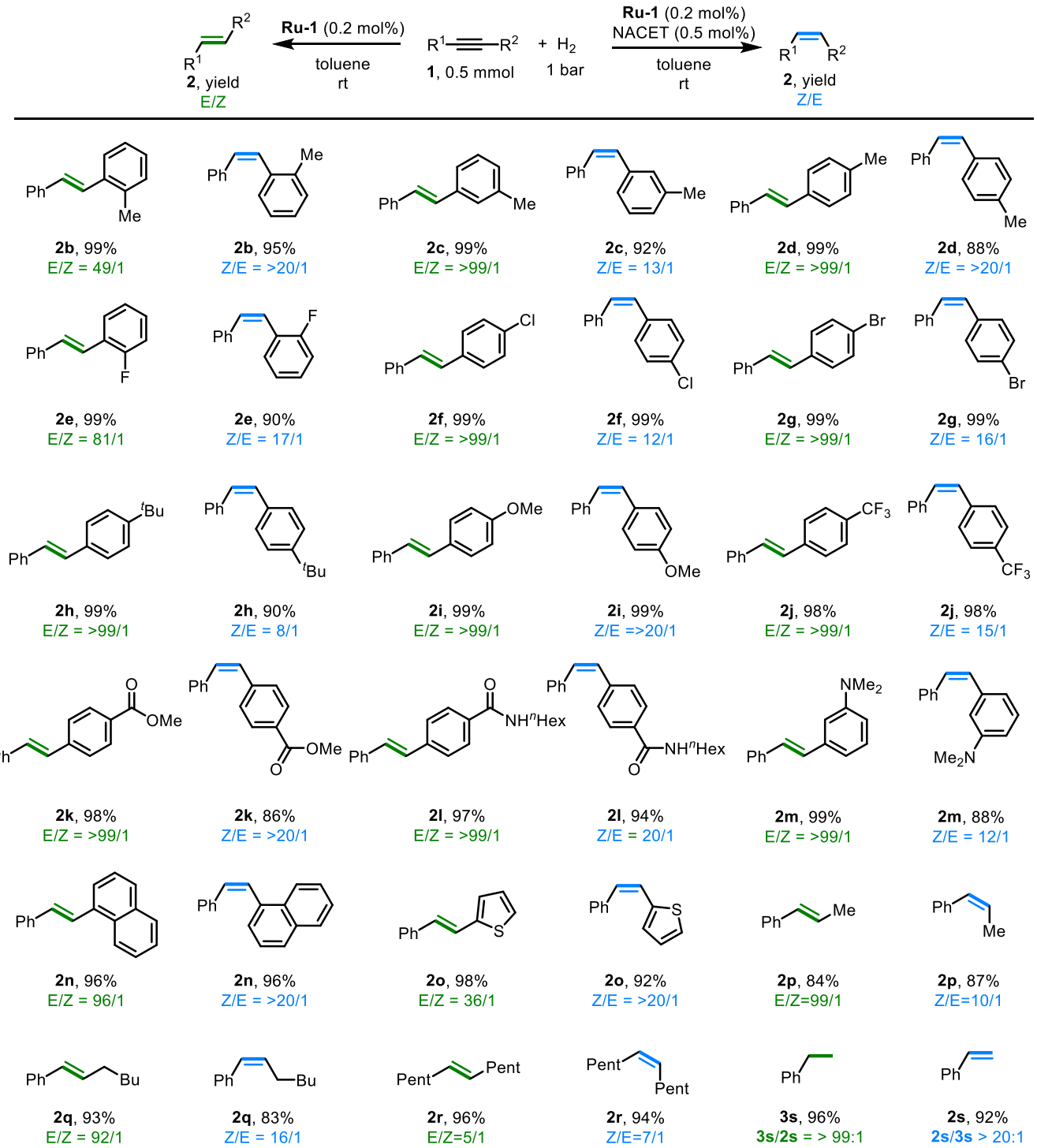

Figure 5. Substrate scope exploration. General conditions: **1** (0.5 mmol), **Ru-1** (0.2 mol%), NACET (0 or 0.5 mol%), toluene (1 mL), H_2 (1 bar), room temperature. Product ratios and yields were determined by ^{1}H NMR spectroscopy using 1,3,5-trimethoxybenezene (0.25 mmol) as an internal standard. See Table S1 for variations in the reaction conditions.

Controllable isomerization of alkenes using amine additives. The current catalytic system was expanded to include the controllable isomerization of alkenes, highlighting the versatility of the reversible inhibition strategy. As mentioned above,

our **Ru-1** complex is also a highly efficient catalyst for the isomerization of C=C double bonds. Thus, when 4-phenyl-1-butene **1t** was employed as substrate under the alkene isomerization conditions, in the absence of H_2 gas (eq. 2), **3-2t** was obtained selectively after 48 h, following C=C bond shift to the 3-position (92% yield, > 20:1 of **3-2t/2-2t**).[71] Interestingly, NACET was found to be too poisonous to allow for efficient isomerization in this case, but the addition of a catalytic amount of $HexNH_2$ to **Ru-1** enabled it to selectively catalyze the isomerization of the C=C bond to the 2-position, affording product **2-2t** in 89% yield (> 20:1 of **2-2t/3-2t**).

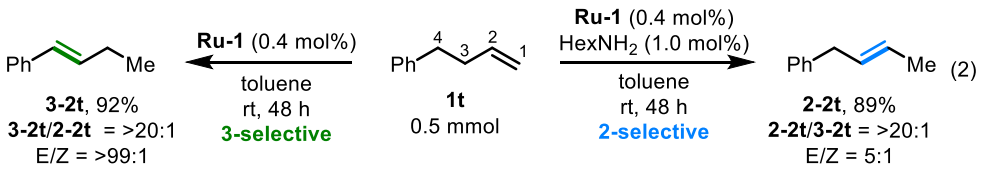

CONCLUSIONS

In conclusion, we have introduced a thiol-enabled controllable H_2-based semihydrogenation of alkynes as a means to afford various alkenes in excellent stereoselectivity, using a single catalytic system involving a ruthenium pincer complex as the catalyst. According to this new methodology, the thiol serves as a switch that adjusts the selectivity of the system, such that the absence of thiol results in the trans-selective semihydrogenation of internal alkynes to give (E)-alkenes, whereas addition of thiol easily halts the reaction at the (Z)-alkene intermediate. Our mechanistic study indicates that the presence of thiol prevents the isomerization of alkenes by blocking the vacant coordination site on the catalyst, while selectively allowing the main process of alkyne hydrogenation to take place through generation of the ruthenium thiol(ate) catalyst. This bioinspired strategy of reversibly protecting the vacant site on the metal center to achieve selective catalysis is expected to have further applications in both homogeneous and heterogeneous catalysis.

EXPERIMENTAL PROCEDURES

Typical procedure for controllable Z/E semihydrogenation of alkynes.

Trans-semihydrogenation of **1a**: In an N_2-filled glovebox, a 90 mL Fischer-Porter tube was charged with alkyne **1a** (0.89 g, 5 mmol), **Ru-1** (2.8 mg, 5.0 µmol), toluene (5 mL) and a stirring bar. The tube was taken out of the glovebox and pressurized with about 2.2 bar of H_2, and the resulting mixture was stirred at 25 °C. After 15 h, the color of the resulting solution changed from red-brown to yellow, with the hydrogen pressure dropping to about 0.8 bar. Subsequently, the excess hydrogen gas was slowly released and the solvent was removed under reduced pressure. The resulting yellow solid was washed with MeOH, resulting in **2a** as a white solid in 96% isolated yield (E/Z > 99:1 detected in the crude mixture; yield of **3a** < 0.1%).

Cis-semihydrogenation of **1a**: In an N_2-filled glovebox, a 90 mL Fischer-Porter tube was charged with alkyne **1a** (0.89 g, 5 mmol), **Ru-1** (2.8 mg, 5.0 µmol), NACET (2.4 mg, 12.5 µmol), toluene (5 mL) and a stirring bar. The tube was taken out of the glovebox and pressurized with about 2.2 bar of H_2, and the resulting mixture was stirred at 25 °C. After 68 h, the hydrogen pressure dropped to 1 bar. Subsequently, the excess hydrogen gas was slowly released and the solvent was removed under reduced pressure. The crude reaction mixture was directly analyzed by NMR spectroscopy, indicating Z/E selectivity of >20:1. This mixture was then dissolved in hexane and passed through a silica column, after which the solvent was removed under reduced pressure to afford a mixture containing the alkenes and unreacted alkyne (84% NMR yield according to the sample weight and peak integrals).

DATA AVAILABILITY

Control experiments, experimental procedures, NMR spectra and computational details are available within this article and its Supplemental Information. The X-ray crystallographic coordinates for the structure reported in this study have been deposited at the Cambridge Crystallographic Data Centre (CCDC), under deposition number 2163250. The data can be obtained free of charge from The Cambridge Crystallographic Data Centre. Any further relevant data are available from the authors upon reasonable request.

SUPPLEMENTAL INFORMATION

Supplemental Information can be found online at https://doi.org/xxxxx/xxxxx.

ACKNOWLEDGMENTS

D.M. is the Israel Matz Professorial Chair of Organic Chemistry, J. L. is thankful to the Feinberg Graduate School of Weizmann Institute of Science for a Senior Postdoctoral Fellowship. We thank Dr. Mark Iron for his help on the computational works.

AUTHOR CONTRIBUTIONS

‡J.L. and Y.L. contributed equally to this work. D.M. and J.L. conceived and directed the project. D.M., J.L. and Y.L. designed the experiments. J.L. and Y.L. performed and analyzed the experiments, and carried out the computational work. Y.D.-P. and L.A. contributed crucial analytical data. D.M., J.L. and M.M. composed the manuscript.

DECLARATION OF INTERESTS

The authors declare no competing interests.

REFERENCES

1. Muller, P. (1994). Glossary of terms used in physical organic chemistry (IUPAC recommendations 1994). Pure Appl. Chem. *66*, 1077-1184.
2. Jacox, M. E. (2002). The spectroscopy of molecular reaction intermediates trapped in the solid rare gases. Chem. Soc. Rev. *31*, 108-115.
3. Srimani, D., Diskin-Posner, Y., Ben-David, Y. and Milstein, D. (2013). Iron pincer complex catalyzed, environmentally benign, E-selective semi-hydrogenation of alkynes. Angew. Chem. Int. Ed. *52*, 14131-14134.
4. Karunananda, M. K. and Mankad, N. P. (2015). E-selective semi-hydrogenation of alkynes by heterobimetallic catalysis. J. Am. Chem. Soc. *137*, 14598-14601.
5. Furukawa, S. and Komatsu, T. (2016). Selective hydrogenation of functionalized alkynes to (E)-alkenes, using ordered alloys as catalysts. ACS Catal. *6*, 2121-2125.
6. Tokmic, K. and Fout, A. R. (2016). Alkyne semihydrogenation with a well-defined nonclassical Co-H_2 catalyst: A H_2 spin on isomerization and E-selectivity. J. Am. Chem. Soc. *138*, 13700-13705.
7. Wang, Y., Huang, Z. and Huang, Z. (2019). Catalyst as colour indicator for endpoint detection to enable selective alkyne trans-hydrogenation with ethanol. Nat. Catal. *2*, 529-536.
8. Yadav, S., Dutta, I., Saha, S., Das, S., Pati, S. K., Choudhury, J. and Bera, J. K. (2020). An annelated mesoionic carbene (MIC) based Ru(II) catalyst for chemo- and stereoselective semihydrogenation of internal and terminal alkynes. Organometallics *39*, 3212-3223.
9. Hale, D. J., Ferguson, M. J. and Turculet, L. (2021). (PSiP)Ni-catalyzed (E)-selective semihydrogenation of alkynes with molecular hydrogen. ACS Catal. *12*, 146-155.
10. Richmond, E. and Moran, J. (2015). Ligand control of E/Z selectivity in nickel-catalyzed transfer hydrogenative alkyne semireduction. J. Org. Chem. 80, 6922-6929.
11. Kusy, R. and Grela, K. (2016). E- and Z-selective transfer semihydrogenation of alkynes catalyzed by standard ruthenium olefin metathesis catalysts. Org. Lett. *18*, 6196-6199.
12. Li, K., Yang, C., Chen, J., Pan, C., Fan, R., Zhou, Y., Luo, Y., Yang, D. and Fan, B. (2021). Anion controlled stereodivergent semi-hydrogenation of alkynes using water as hydrogen source. Asian J. Org. Chem. *10*, 2143-2146.
13. Yang, J., Wang, C., Sun, Y., Man, X., Li, J. and Sun, F. (2019). Ligand-controlled iridium-catalyzed semihydrogenation of alkynes with ethanol: Highly stereoselective synthesis of E- and Z-alkenes. Chem. Commun. *55*, 1903-1906.
14. Rao, S. and Prabhu, K. R. (2018). Stereodivergent alkyne reduction by using water as the hydrogen source. Chem. Eur. J. *24*, 13954-13962.
15. Fu, S., Chen, N. Y., Liu, X., Shao, Z., Luo, S. P. and Liu, Q. (2016). Ligand-controlled cobalt-catalyzed transfer hydrogenation of alkynes: Stereodivergent synthesis of Z- and E-alkenes. J. Am. Chem. Soc. *138*, 8588-8594.
16. Li, K., Khan, R., Zhang, X., Gao, Y., Zhou, Y., Tan, H., Chen, J. and Fan, B. (2019). Cobalt catalyzed stereodivergent semi-hydrogenation of alkynes using H_2O as the hydrogen source. Chem. Commun. *55*, 5663-5666.
17. Luo, F., Pan, C., Wang, W., Ye, Z. and Cheng, J. (2010). Palladium-catalyzed reduction of alkynes employing $HSiEt_3$: Stereoselective synthesis of trans- and cis-alkenes. Tetrahedron 66, 1399-1403.
18. Li, J. and Hua, R. (2011). Stereodivergent ruthenium-catalyzed transfer semihydrogenation of diaryl alkynes. Chem. Eur. J. *17*, 8462-8465.
19. Shen, R., Chen, T., Zhao, Y., Qiu, R., Zhou, Y., Yin, S., Wang, X., Goto, M. and Han, L. B. (2011). Facile regio- and stereoselective hydrometalation of alkynes with a combination of carboxylic acids and group 10 transition metal complexes: Selective hydrogenation of alkynes with formic acid. J. Am. Chem. Soc. *133*, 17037-17044.
20. Chen, K., Zhu, H., Li, Y., Peng, Q., Guo, Y. and Wang, X. (2021). Dinuclear cobalt complex-catalyzed stereodivergent semireduction of alkynes: Switchable selectivities controlled by H_2O. ACS Catal. *11*, 13696-13705.
21. Vahrenkamp, H. (1975). Sulfur atoms as ligands in metal complexes. Angew. Chem. Int. Ed. *14*, 322-329.
22. Gargir, M., Ben-David, Y., Leitus, G., Diskin-Posner, Y., Shimon, L. J. W. and Milstein, D. (2012). PNS-type ruthenium pincer complexes. Organometallics *31*, 6207-6214.
23. Nasaruddin, R. R., Chen, T., Yan, N. and Xie, J. (2018). Roles of thiolate ligands in the synthesis, properties and catalytic application of gold nanoclusters. Coord. Chem. Rev. *368*, 60-79.
24. Gennari, M. and Duboc, C. (2020). Bio-inspired, multifunctional metal-thiolate motif: From electron transfer to sulfur reactivity and small-molecule activation. Acc. Chem. Res. *53*, 2753-2761.
25. Siemann, S., Clarke, A. J., Viswanatha, T. and Dmitrienko, G. I. (2003). Thiols as classical and slow-binding inhibitors of IMP-1 and other binuclear metallo-β-lactamases. Biochemistry *42*, 1673-1683.
26. Bahr, G., Gonzalez, L. J. and Vila, A. J. (2021). Metallo-beta-lactamases in the age of multidrug resistance: From structure and mechanism to evolution, dissemination, and inhibitor design. Chem. Rev. *121*, 7957-8094.
27. Yee, K. K., Reimer, N., Liu, J., Cheng, S. Y., Yiu, S. M., Weber, J., Stock, N. and Xu, Z. (2013). Effective mercury sorption by thiol-laced metal-organic frameworks: In strong acid and the vapor phase. J. Am. Chem. Soc. *135*, 7795-7798.
28. Wang, K., Peng, H. and Wang, B. (2014). Recent advances in thiol and

sulfide reactive probes. J. Cell. Biochem. *115*, 1007-1022.
29. Bjorklund, G., Crisponi, G., Nurchi, V. M., Cappai, R., Buha Djordjevic, A. and Aaseth, J. (2019). A review on coordination properties of thiol-containing chelating agents towards mercury, cadmium, and lead. Molecules *24*, 3247.
30. Vericat, C., Vela, M. E., Benitez, G., Carro, P. and Salvarezza, R. C. (2010). Self-assembled monolayers of thiols and dithiols on gold: New challenges for a well-known system. Chem. Soc. Rev. *39*, 1805-1834.
31. Vericat, C., Vela, M. E., Corthey, G., Pensa, E., Cortés, E., Fonticelli, M. H., Ibañez, F., Benitez, G. E., Carro, P. and Salvarezza, R. C. (2014). Self-assembled monolayers of thiolates on metals: A review article on sulfur-metal chemistry and surface structures. RSC. Adv. *4*, 27730-27754.
32. Kuniyasu, H., Ogawa, A., Sato, K., Ryu, I., Kambe, N. and Sonoda, N. (1992). The first example of transition-metal-catalyzed addition of aromatic thiols to acetylenes. J. Am. Chem. Soc. *114*, 5902-5903.
33. Itoh, T. and Mase, T. (2006). Practical thiol surrogates and protective groups for arylthiols for Suzuki-Miyaura conditions. J. Org. Chem. *71*, 2203-2206.
34. Zeysing, B., Gosch, C. and Terfort, A. (2000). Protecting groups for thiols suitable for Suzuki conditions. Org. Lett. *2*, 1843-1845.
35. Gui, B., Yee, K. K., Wong, Y. L., Yiu, S. M., Zeller, M., Wang, C. and Xu, Z. (2015). Tackling poison and leach: Catalysis by dangling thiol-palladium functions within a porous metal-organic solid. Chem. Commun. *51*, 6917-6920.
36. Luo, J., Rauch, M., Avram, L., Ben-David, Y. and Milstein, D. (2020). Catalytic hydrogenation of thioesters, thiocarbamates, and thioamides. J. Am. Chem. Soc. *142*, 21628-21633.
37. Chauhan, B. P., Rathore, J. S. and Bandoo, T. (2004). "Polysiloxane-Pd" nanocomposites as recyclable chemoselective hydrogenation catalysts. J. Am. Chem. Soc. *126*, 8493-8500.
38. Panthi, B., Mukhopadhyay, A., Tibbitts, L., Saavedra, J., Pursell, C. J., Rioux, R. M. and Chandler, B. D. (2015). Using thiol adsorption on supported au nanoparticle catalysts to evaluate au dispersion and the number of active sites for benzyl alcohol oxidation. ACS Catal. *5*, 2232-2241.
39. Inkpen, M. S., Liu, Z. F., Li, H., Campos, L. M., Neaton, J. B. and Venkataraman, L. (2019). Non-chemisorbed gold-sulfur binding prevails in self-assembled monolayers. Nat .Chem. *11*, 351-358.
40. Makosch, M., Lin, W.-I., Bumbálek, V., Sá, J., Medlin, J. W., Hungerbühler, K. and van Bokhoven, J. A. (2012). Organic thiol modified Pt/TiO_2 catalysts to control chemoselective hydrogenation of substituted nitroarenes. ACS Catal. *2*, 2079-2081.
41. Kahsar, K. R., Schwartz, D. K. and Medlin, J. W. (2014). Control of metal catalyst selectivity through specific noncovalent molecular interactions. J. Am. Chem. Soc. *136*, 520-526.
42. Pang, S. H., Schoenbaum, C. A., Schwartz, D. K. and Medlin, J. W. (2014). Effects of thiol modifiers on the kinetics of furfural hydrogenation over Pd catalysts. ACS Catal. *4*, 3123-3131.
43. Zhang, Y., Wen, X., Shi, Y., Yue, R., Bai, L., Liu, Q. and Ba, X. (2018). Sulfur-containing polymer as a platform for synthesis of size-controlled pd nanoparticles for selective semihydrogenation of alkynes. Ind. Eng. Chem. Res. *58*, 1142-1149.
44. Yoshii, T., Umemoto, D., Kuwahara, Y., Mori, K. and Yamashita, H. (2019). Engineering of surface environment of Pd nanoparticle catalysts on carbon support with pyrene-thiol ligands for semihydrogenation of alkynes. ACS Appl. Mater. Interfaces *11*, 37708-37719.
45. San, K. A. and Shon, Y. S. (2018). Synthesis of alkanethiolate-capped metal nanoparticles using alkyl thiosulfate ligand precursors: A method to generate promising reagents for selective catalysis. Nanomaterials *8*, 346.
46. Zhao, X., Zhou, L., Zhang, W., Hu, C., Dai, L., Ren, L., Wu, B., Fu, G. and Zheng, N. (2018). Thiol treatment creates selective palladium catalysts for semihydrogenation of internal alkynes. Chem *4*, 1080-1091.
47. Lindlar, H. (1966). Palladium catalyst for partial reduction of acetylenes. Org. Syn. *46*, 446-450.
48. Crespo-Quesada, M., Cárdenas-Lizana, F., Dessimoz, A.-L. and Kiwi-Minsker, L. (2012). Modern trends in catalyst and process design for alkyne hydrogenations. ACS Catal. *2*, 1773-1786.
49. Radkowski, K., Sundararaju, B. and Furstner, A. (2013). A functional-group-tolerant catalytic trans hydrogenation of alkynes. Angew. Chem. Int. Ed. *52*, 355-360.
50. Slack, E. D., Gabriel, C. M. and Lipshutz, B. H. (2014). A palladium nanoparticle-nanomicelle combination for the stereoselective semihydrogenation of alkynes in water at room temperature. Angew. Chem. Int. Ed. *53*, 14051-14054.
51. Frihed, T. G. and Fürstner, A. (2016). Progress in the trans-reduction and trans-hydrometalation of internal alkynes. Applications to natural product synthesis. Bull. Chem. Soc. Jpn. *89*, 135-160.
52. Zhong, J. J., Liu, Q., Wu, C. J., Meng, Q. Y., Gao, X. W., Li, Z. J., Chen, B., Tung, C. H. and Wu, L. Z. (2016). Combining visible light catalysis and transfer hydrogenation for in situ efficient and selective semihydrogenation of alkynes under ambient conditions. Chem. Commun. *52*, 1800-1803.
53. Delgado, J. A., Benkirane, O., Claver, C., Curulla-Ferre, D. and Godard, C. (2017). Advances in the preparation of highly selective nanocatalysts for the semi-hydrogenation of alkynes using colloidal approaches. Dalton Trans. *46*, 12381-12403.
54. Tejeda-Serrano, M., Cabrero-Antonino, J. R., Mainar-Ruiz, V., López-Haro, M., Hernández-Garrido, J. C., Calvino, J. J., Leyva-Pérez, A. and Corma, A. (2017). Synthesis of supported planar iron oxide nanoparticles and their chemo- and stereoselectivity for hydrogenation of alkynes. ACS Catal. *7*, 3721-3729.
55. Swamy, K. C. K., Reddy, A. S., Sandeep, K. and Kalyani, A. (2018). Advances in chemoselective and/or stereoselective semihydrogenation of alkynes. Tetrahedron Lett. *59*, 419-429.
56. Furstner, A. (2019). Trans-hydrogenation, *gem*-hydrogenation, and trans-hydrometalation of alkynes: An interim report on an unorthodox reactivity paradigm. J. Am. Chem. Soc. *141*, 11-24.
57. Gorgas, N., Brunig, J., Stoger, B., Vanicek, S., Tilset, M., Veiros, L. F. and Kirchner, K. (2019). Efficient Z-selective semihydrogenation of internal alkynes catalyzed by cationic iron(II) hydride complexes. J. Am. Chem. Soc. *141*, 17452-17458.
58. Decker, D., Drexler, H.-J., Heller, D. and Beweries, T. (2020). Homogeneous catalytic transfer semihydrogenation of alkynes-An

overview of hydrogen sources, catalysts and reaction mechanisms. Catal. Sci. Technol. *10*, 6449-6463.
59. Garbe, M., Budweg, S., Papa, V., Wei, Z., Hornke, H., Bachmann, S., Scalone, M., Spannenberg, A., Jiao, H., Junge, K. and Beller, M. (2020). Chemoselective semihydrogenation of alkynes catalyzed by manganese(I)-PNP pincer complexes. Catal. Sci. Technol. *10*, 3994-4001.
60. Ramirez, B. L. and Lu, C. C. (2020). Rare-earth supported nickel catalysts for alkyne semihydrogenation: Chemo- and regioselectivity impacted by the Lewis acidity and size of the support. J. Am. Chem. Soc. *142*, 5396-5407.
61. Sharma, D. M. and Punji, B. (2020). 3 d transition metal-catalyzed hydrogenation of nitriles and alkynes. Chem. Asian. J. *15*, 690-708.
62. Tang, S., Rauch, M., Montag, M., Diskin-Posner, Y., Ben-David, Y. and Milstein, D. (2020). Catalytic oxidative deamination by water with H_2 liberation. J. Am. Chem. Soc. *142*, 20875-20882.
63. Kar, S., Rauch, M., Leitus, G., Ben-David, Y. and Milstein, D. (2021). Highly efficient additive-free dehydrogenation of neat formic acid. Nat. Catal. *4*, 193-201.
64. Luo, J., Rauch, M., Avram, L., Diskin-Posner, Y., Shmul, G., Ben-David, Y. and Milstein, D. (2020). Formation of thioesters by dehydrogenative coupling of thiols and alcohols with H_2 evolution. Nat. Catal. *3*, 887-892.
65. Luo, J., Kar, S., Rauch, M., Montag, M., Ben-David, Y. and Milstein, D. (2021). Efficient base-free aqueous reforming of methanol homogeneously catalyzed by ruthenium exhibiting a remarkable acceleration by added catalytic thiol. J. Am. Chem. Soc. *143*, 17284-17291.
66. Rauch, M., Luo, J., Avram, L., Ben-David, Y. and Milstein, D. (2021). Mechanistic investigations of ruthenium catalyzed dehydrogenative thioester synthesis and thioester hydrogenation. ACS Catal. *11*, 2795-2807.
67.Zhu, Q. and Nocera, D. G. (2021). Catalytic C(β)–O bond cleavage of lignin in a one-step reaction enabled by a spin-center shift. ACS Catal. *11*, 14181-14187.
68. Diemer, V., Firstova, O., Agouridas, V. and Melnyk, O. (2022). Pedal to the metal: The homogeneous catalysis of the native chemical ligation reaction. Chem. Eur. J. *28*, e202104229.
69. Ye, X., Plessow, P. N., Brinks, M. K., Schelwies, M., Schaub, T., Rominger, F., Paciello, R., Limbach, M. and Hofmann, P. (2014). Alcohol amination with ammonia catalyzed by an acridine-based ruthenium pincer complex: A mechanistic study. J. Am. Chem. Soc. *136*, 5923-5929.
70. Gellrich, U., Khusnutdinova, J. R., Leitus, G. M. and Milstein, D. (2015). Mechanistic investigations of the catalytic formation of lactams from amines and water with liberation of H_2. J. Am. Chem. Soc. *137*, 4851-4859.
71. Camp, A. M., Kita, M. R., Blackburn, P. T., Dodge, H. M., Chen, C. H. and Miller, A. J. M. (2021). Selecting double bond positions with a single cation-responsive iridium olefin isomerization catalyst. J. Am. Chem. Soc. *143*, 2792-2800.